Book: Desiderata Geotechnica
Year: 2019

On the Simulation of the Cyclic Mobility Effect with an ISA-Hypoplastic Model

W. Fuentes(✉) and C. Lascarro

University del Norte, Barranquilla, Colombia
{fuentesw,cjlascarro}@uninorte.edu.co

Abstract. The ISA-Hypoplasticity corresponds to an extended version of conventional Hypoplasticity to enable the simulation of some observed effects on cyclic loading. This extension offers novel features compared to the intergranular strain theory by Herle and Niemunis [4], including the incorporation of an elastic strain amplitude, to separate the elastic and plastic response, and the ability to reduce the plastic accumulation rate upon a larger number of cycles ($N > 10$). In the present work, a modification to the ISA-hypoplastic model is described in order to enable the simulation of cyclic mobility effects exhibited by granular materials. The modification is based on a new state variable, able to detect paths at which the cyclic mobility effect is activated. With this information, some factors of the ISA-hypoplastic model are modified to deliver the proper response on paths showing cyclic mobility effects. Simulations examples are given to illustrate the new mechanism and a short analysis of the new parameters is also included.

1 Introduction

The Intergranular Strain Anisotropy (ISA) can be considered as a mathematical extension of conventional Hypoplasticity for sands [9] or clays [3,7], to improve cyclic loading simulations. Originally, it was proposed to consider three observed effects on cyclic paths [2]: a strain amplitude dividing the plastic and elastic regime, the increase of the stiffness upon reversal loading and the reduction of the plastic strain rate under the same conditions. Successful simulations of cyclic loading for a low number of cycles ($N < 10$) were achieved [2]. Nevertheless, some inspections on the formulation revealed the weakness of the model to predict the behavior of the accumulated plastic behavior upon a higher number of repetitive cycles ($N > 10$). This motivated Poblete et al. [5] to modify the model to account for the effect of repetitive cycles. For a large number of cycles ($N > 10$), the new relations were now able to simulate the observed reduction of the plastic accumulation rate, and showed to work well, not only on undrained cyclic triaxial tests, but also on complex multidimensional cyclic loading under drained conditions [5]. Despite of all these achievements, some issues related to the absence of cyclic mobility effects, and thus the liquefaction analysis, were not addressed by the existent relations given the fact, that this effect were considered to be related to the reference hypoplastic equation, and not to the extension provided by ISA. As a matter of fact, despite the vast amount of works studying hypoplastic models under several cyclic tests, scarce works are devoted to propose relations encompassing the cyclic mobility effect.

The current work describes an extension of an ISA-hypoplastic model to enable the simulation of the cyclic mobility effect, and thus to permit the analysis of liquefaction under undrained conditions. To that end, a strain-type sate variable $\mathbf{z}$ is introduced to detect paths at which the cyclic mobility effect is activated. This information is then considered to modify some factors of the constitutive equation. It will be shown, that the modifications presented herein permit the simulation of cyclic mobility, without altering other former capabilities of hypoplastic models related to the stress-dilatancy behavior under drained conditions.

2 New Modifications of the ISA-Hypoplastic Model

The equations of the reference model are described in the appendices. It corresponds to the Hypoplastic equation by Wollfersdorff [9] extended by the ISA relations according to [2,5]. Evaluation of the model capabilities under cyclic loading can be found in [5]. Its extension to consider cyclic mobility effects is described in the following lines.

In order to detect paths at which the cyclic mobility effect is activated, we introduce a new state variable, denoted with $\mathbf{z}$, with an evolution equation similar to [1]:

$$\dot{\mathbf{z}} = c_z \langle \eta/(M_c f_{d0} F) - 1 \rangle (\mathbf{N} - \mathbf{z}) \|\dot{\boldsymbol{\varepsilon}}\| \tag{1}$$

whereby c_z is a new material parameter controlling the rate of $\mathbf{z}$, $M_c = 6\sin(\varphi_c)/(3 - \sin\varphi_c)$ is the critical state slope, $\eta = q/p$ is the stress ratio, and the factors F and f_{d0} are scalar functions, the first described in the appendices, and the second defined in the sequel. Let denote z the scalar function defined as:

$$z = \langle \mathbf{z} : \mathbf{N} \rangle \tag{2}$$

where $\mathbf{N}$ is a unit tensor ($\|\mathbf{N}\| = 1$) providing information about the intergranular strain rate direction, see Eq. 8. According to Eq. 2, factor z is bounded by $0 \leq z \leq 1$. A value of $z = 0$ indicates that the effect of the cyclic mobility is not accounted by the model, while a value of $z = 1$ means that it is fully considered. Intermediate values of $0 < z < 1$ intend to simulate a transition between these two states. For the case of $z = 1$, we propose that the model reproduces a contractant behavior as by looses states $e \approx e_c$. Specifically, we propose to consider the following characteristics:

- For $z = 1$, the scalar factors f_e and f_d are set to one, i.e. $f_e = f_d = 1$. This is equivalently to evaluate these factors at $e = e_c$.
- For the same condition ($z = 1$), the strain amplitude $\Delta\boldsymbol{\varepsilon}$ at which the intergranular strain effect is reproduced is reduced.

The first requirement is considered through the introduction of the following modifications to the scalar factors f_e and f_d:

$$f_e = f_{e0} - z\langle f_{e0} - 1\rangle, \quad \text{with} \quad f_{e0} = \left(\frac{e_c}{e}\right)^{\beta} \tag{3}$$

$$f_d = f_{d0} + z\langle 1 - f_{d0}\rangle, \quad \text{with} \quad f_{d0} = \left(\frac{e - e_d}{e_c - e_d}\right)^{\alpha} \tag{4}$$

Note that for $z = 1$, they give $f_e = f_d = 1$. For the second requirement, we propose that the former parameter β_h is converted into a function:

$$\beta_h = \beta_{\max} + (\beta_0 - \beta_{\max})(1 - z) \tag{5}$$

which now depends on parameters β_0 and $\beta_{\max}$. For $z = 0$, it gives $\beta_h = \beta_0$, coinciding with its original definition. On the other hand, the relation $\beta_h = \beta_{\max}$ holds for $z = 1$ conditions. At that state ($z = 1$), the new parameter $\beta_{\max}$ allows to control the strain amplitude $\|\Delta\boldsymbol{\varepsilon}\|$ at which the intergranular strain effect is considered. Hence, simulation of the cyclic mobility effect requires the calibration of the new parameters c_z and $\beta_{\max}$.

We now present some simulations examples. The Karlsruhe fine sand parameters reported in [5] are borrowed for the following simulations ($e_{\max} = 1.054$, $e_{\min} = 0.677$). Consider a drained triaxial test with constant mean pressure $p =$ constant, such as the tests by [6]. The test is performed under $p = 100\,\text{kPa}$ (constant), with an initial void ratio of $e_0 = 0.6$ (dense state). Three different simulations are presented in Fig. 1, whereby the variation of the parameter $c_z = \{0, 100, 300\}$ is considered. From the results one may see, that for higher values of c_z, a higher degradation of the shear stiffness accompanied with an increase of the compressive volumetric strains are obtained. Hence, c_z may be calibrated by trial and error, to provide accurate simulations of these effects under cycles of large strain amplitudes ($\|\Delta\boldsymbol{\varepsilon}\| > 0.001$). Notice that the stress-dilatancy response exhibited in Fig. 1d, is not spoiled by the current modification.

A cyclic undrained triaxial test with constant deviator stress amplitude ($q^{\text{amp}} = 40\,\text{kPa}$) is shown in Fig. 2. For this simulation, c_z is set to $c_z = 300$. The results show that the model is able to reproduce the cyclic mobility effect observed on the last cycles. This is better noted on Fig. 3, whereby the simulation of the reference model lacking of the current extension is included. The proposed extension assesses to simulate the "butterfly-type" paths in the $p - q$, see Fig. 3a, while the accumulation of the pore water pressure p_w upon the number of cycles N is well reproduced, see Fig. 3b.

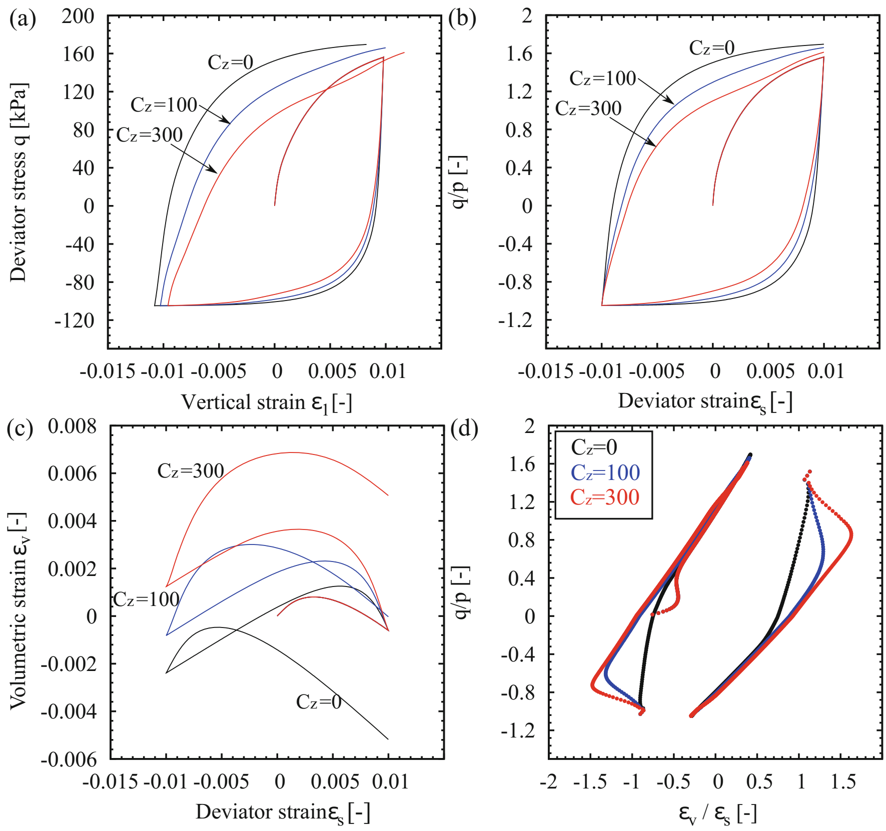

Fig. 1. Simulation of a $p = \text{const}$ triaxial test under drained conditions. Karlsruhe fine sand parameters. $p = 100\,\text{kPa}$.

Closure

The present work described an extended version of the ISA-hypoplastic model able to simulate cyclic mobility effects. To that end, an additional state variable **z** has been introduced, able to detect paths at which the cyclic mobility effect is activated. This information is used on factors f_e and f_d of the hypoplastic model, and on factor β_h from the ISA model. The proposed methodology requires the calibration of two parameters, namely, c_z which controls the rate of **z** and $\beta_{\max}$ controlling the strain amplitude upon cyclic mobility wherein the intergranular strain influences the response. The current extension is simple, and provides fair simulations of cyclic undrained tests while keeping its capabilities on the stress-dilatancy response under drained conditions.

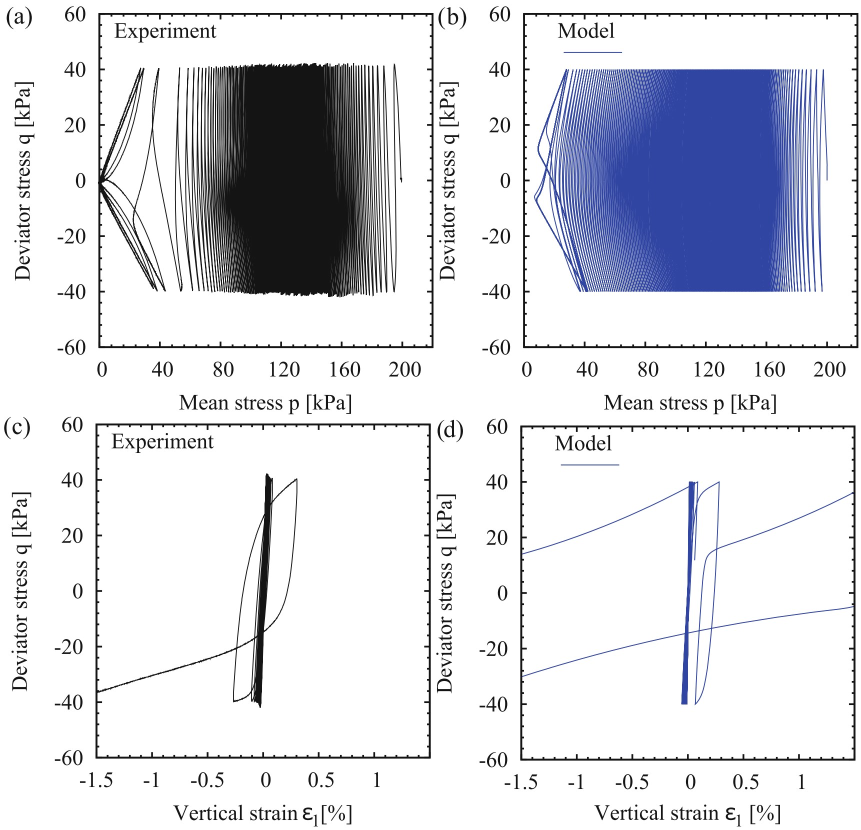

Fig. 2. Simulation of a cyclic undrained triaxial test. Deviator stress amplitude of $q^{\text{amp}} = 40\,\text{kPa}$. Experiment using Karlsruhe fine sand, data by [8]

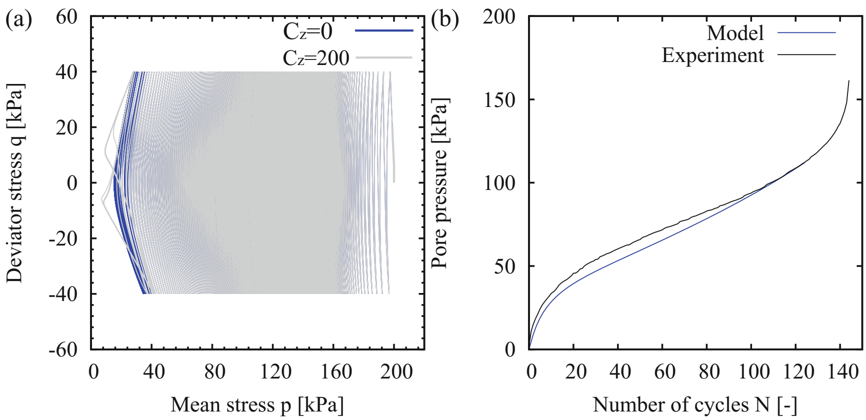

Fig. 3. Accumulated pore pressure p_w against number of cycles N. Parameters of Karlruhe fine sand

Notation and Conventions

The notation and convention of the present work is as follows: italic fonts denote scalar magnitudes (e.g. a, b), bold lowercase letters denote vectors (e.g. $\mathbf{a}, \mathbf{b}$), bold capital letters denote second-rank tensors (e.g. $\mathbf{A}, \boldsymbol{\sigma}$), and special fonts are used for fourth-rank tensors (e.g. E, L). Indicial notation can be used to represent components of tensors (e.g. A_{ij}), and their operations follow the Einstein's summation convention. The Kronecker delta symbol is represented by δ_{ij}, i.e. $\delta_{ij} = 1$ when $i = j$ and $\delta_{ij} = 0$ otherwise. The symbol $\mathbf{1}$ denotes the Kronecker delta tensor ($1_{ij} = \delta_{ij}$). The unit fourth-rank tensor for symmetric tensors is denoted by I, where $\mathsf{I}_{ijkl} = \frac{1}{2}\left(\delta_{ik}\delta_{jl} + \delta_{il}\delta_{jk}\right)$. Multiplication with two dummy indices (double contraction) is denoted with a colon ":" (e.g. $\mathbf{A} : \mathbf{B} = A_{ij}B_{ij}$). The symbol "$\otimes$" represents the dyadic product (e.g. $\mathbf{A} \otimes \mathbf{B} = A_{ij}B_{kl}$). The brackets $\| \sqcup \|$ extract the Euclidean norm (e.g. $\| \mathbf{A} \| = \sqrt{A_{ij}A_{ij}}$). Normalized tensors are denoted by $\overrightarrow{\sqcup} = \frac{\sqcup}{\|\sqcup\|}$, or in general as $\sqcup^{\rightarrow}$. The superscript $\sqcup^{\text{dev}}$ extracts the deviatoric part of a tensor (e.g. $\mathbf{A}^{\text{dev}} = \mathbf{A} - \frac{1}{3}(\text{tr}\mathbf{A})\mathbf{1}$). Components of the effective stress tensor $\boldsymbol{\sigma}$ or strain tensor $\boldsymbol{\varepsilon}$ in compression are negative. Roscoe variables are defined as $p = -\sigma_{ii}/3$, $q = \sqrt{\frac{3}{2}}\|\boldsymbol{\sigma}^{\text{dev}}\|$, $\varepsilon_v = -\varepsilon_{ii}$ and $\varepsilon_s = \sqrt{\frac{2}{3}}\|\boldsymbol{\varepsilon}^{\text{dev}}\|$. The stress ratio η is defined as $\eta = q/p$. The deviator stress tensor is defined as $\boldsymbol{\sigma}^{\text{dev}} = \boldsymbol{\sigma} + p\,\mathbf{1}$ and the stress-ratio tensor with $\mathbf{r} = \boldsymbol{\sigma}^{\text{dev}}/p = \sqrt{\frac{2}{3}}\,\eta\,\overrightarrow{\boldsymbol{\sigma}^{\text{dev}}}$.

Appendix 1

Appendix 1 presents a summary of the constitutive equations of the ISA-hypoplastic model. Details of the equations below are found in [2,5,9].

$$\dot{\boldsymbol{\sigma}} = \mathsf{M} : \dot{\boldsymbol{\varepsilon}} \tag{6}$$

$$\mathsf{M} = \begin{cases} [m_R + (1 - m_R)y_h](\mathsf{L}^{\text{hyp}} + \rho^{\chi}\mathbf{N}^{\text{hyp}} \otimes \mathbf{N}) & \text{for } F_H \geq 0 \\ m_R \mathsf{L}^{\text{hyp}} & \text{for } F_H < 0 \end{cases} \tag{7}$$

$$\dot{\mathbf{h}} = \dot{\varepsilon} - \dot{\lambda}_H \mathbf{N}, \quad \text{with} \quad \mathbf{N} = \frac{\mathbf{h} - \mathbf{c}}{R/2} \tag{8}$$

$$\dot{\lambda}_H = \frac{\langle \mathbf{N} \colon \dot{\varepsilon} \rangle}{1 - \left(\dfrac{\partial F_H}{\partial \mathbf{c}}\right) : \bar{\mathbf{c}}} \tag{9}$$

$$\dot{\mathbf{c}} = \dot{\lambda}_H \bar{\mathbf{c}}, \quad \text{with} \quad \bar{\mathbf{c}} = \beta_h(\mathbf{c}_b - \mathbf{c})/R, \quad \text{and} \quad \mathbf{c}_b = (R/2)\,\overrightarrow{\dot{\boldsymbol{\varepsilon}}} \tag{10}$$

$$\rho = 1 - \frac{\|\mathbf{h}_b - \mathbf{h}\|}{2R}, \quad \text{with} \quad \mathbf{h}_b = R\mathbf{N} \tag{11}$$

$$y_h = \rho^{\chi} \langle \mathbf{N} \colon \overrightarrow{\dot{\boldsymbol{\varepsilon}}} \rangle \tag{12}$$

$$m = m_R + (1 - m_R) y_h \tag{13}$$

$$\dot{\varepsilon}_{\rm acc} = \frac{C_a}{R}(1 - y_h - \varepsilon_{\rm acc})\|\dot{\boldsymbol{\varepsilon}}\| \tag{14}$$

$$\chi = \chi_0 + \varepsilon_{\rm acc}(\chi_{\max} - \chi_0) \tag{15}$$

The set of parameters are R, χ_0, $\chi_{\max}$, m_R, β_0, $\beta_{\max}$ and C_a.

Appendix 2

In the present appendix, the remaining equations of the reference hypoplastic model [9] are given:

$$\mathsf{L}^{\rm hyp} = f_b f_e \frac{1}{\hat{\boldsymbol{\sigma}} : \hat{\boldsymbol{\sigma}}}(F^2 \mathsf{I} + a^2 \hat{\boldsymbol{\sigma}} \hat{\boldsymbol{\sigma}}) \tag{16}$$

$$\mathbf{N}^{\rm hyp} = f_d f_b f_e \frac{Fa}{\hat{\boldsymbol{\sigma}} : \hat{\boldsymbol{\sigma}}}(\hat{\boldsymbol{\sigma}} + \hat{\boldsymbol{\sigma}}^{\rm dev}) \tag{17}$$

$$\begin{aligned} f_e &= \left(\frac{e_c}{e}\right)^{\beta} \\ f_b &= \frac{h_s}{n_B}\left(\frac{1+e_i}{e_i}\right)\left(\frac{e_{i0}}{e_{c0}}\right)^{\beta}\left(-\frac{\mathrm{tr}\boldsymbol{\sigma}}{h_s}\right)^{1-n_B}\left[3 + a^2 - \sqrt{3}a\left(\frac{e_{i0}-e_{d0}}{e_{c0}-e_{d0}}\right)^{\beta}\right]^{-1} \\ f_d &= \left(\frac{e-e_d}{e_c-e_d}\right)^{\alpha} \end{aligned} \tag{18}$$

$$F = \sqrt{\frac{1}{8}\tan^2(\psi) + \frac{2-\tan^2(\psi)}{2+2\sqrt{2}\tan(\psi)\cos(3\theta)}} - \frac{1}{2\sqrt{2}\tan(\psi)} \tag{19}$$

$$\begin{aligned} a &= \frac{\sqrt{3}(3-\sin(\varphi_c))}{2\sqrt{2}\sin(\varphi_c))} \\ \tan\psi &= \sqrt{3}\|\hat{\boldsymbol{\sigma}}^{\rm dev}\| \\ \cos(3\theta) &= \sqrt{6}\frac{\mathrm{tr}(\hat{\boldsymbol{\sigma}}^{\rm dev}\hat{\boldsymbol{\sigma}}^{\rm dev}\hat{\boldsymbol{\sigma}}^{\rm dev})}{(\hat{\boldsymbol{\sigma}}^{\rm dev} : \hat{\boldsymbol{\sigma}}^{\rm dev})^{3/2}} \end{aligned} \tag{20}$$

$$\begin{aligned} e_i &= e_{i0}\exp\left(-(3p/h_s)^{n_B}\right) \\ e_d &= e_{d0}\exp\left(-(3p/h_s)^{n_B}\right) \\ e_c &= e_{c0}\exp\left(-(3p/h_s)^{n_B}\right) \end{aligned} \tag{21}$$

The set of parameters are φ_c, h_s, n_B, e_{i0}, e_{c0}, e_{d0}, α and β.

References

1. Dafalias, Y., Manzari, M.: Simple plasticity sand model accounting for fabric change effects. J. Eng. Mech. ASCE **130**(6), 622–634 (2004)
2. Fuentes, W., Triantafyllidis, T.: ISA model: a constitutive model for soils with yield surface in the intergranular strain space. Int. J. Numer. Anal. Meth. Geomech. **39**(11), 1235–1254 (2015)
3. Mašín, D.: A hypoplastic constitutive model for clays. Int. J. Numer. Anal. Meth. Geomech. **29**(4), 311–336 (2005)
4. Niemunis, A., Herle, I.: Hypoplastic model for cohesionless soils with elastic strain range. Mech. Cohesive-frictional Mater. **2**(4), 279–299 (1997)
5. Poblete, M., Fuentes, W., Triantafyllidis, T.: On the simulation of multidimensional cyclic loading with intergranular strain. Acta Geotech. **11**(6), 1263–1285 (2016)
6. Pradhan, T., Tatsuoka, F., Sato, Y.: Experimental stress-dilatancy relations of sand subjected to cyclic loading. Soils Found. **29**(1), 45–64 (1989)
7. Weifner, T., Kolymbas, D.: A hypoplastic model for clay and sand. Acta Geotech. **2**(2), 103–112 (2007)
8. Wichtmann, T.: Karlsruhe fine sand data-base. Technical report, Institute of Soil and Rock Mechanics (IBF). Karlsruhe Institute of Technology (KIT) (2015). http://www.torsten-wichtmann.de
9. Wolffersdorff, V.: A hypoplastic relation for granular materials with a predefined limit state surface. Mech. Cohesive-frictional Mater. **1**(3), 251–271 (1996)